

# Human replication protein A can suppress the intrinsic *in vitro* mutator phenotype of human DNA polymerase $\lambda$

Giovanni Maga<sup>1,2,\*</sup>, Igor Shevelev<sup>2</sup>, Giuseppe Villani<sup>3</sup>, Silvio Spadari<sup>1</sup> and Ulrich Hübscher<sup>2</sup>

<sup>1</sup>Istituto di Genetica Molecolare IGM-CNR, Pavia, Italy, <sup>2</sup>Institute of Veterinary Biochemistry and Molecular Biology, University of Zurich-Irchel, Zurich, Switzerland and <sup>3</sup>Institut de Pharmacologie et de Biologie Structurale, IPBS-CNRS, Centre National de la Recherche Scientifique, Toulouse, France

Received January 3, 2006; Revised January 31, 2006; Accepted February 20, 2006

## ABSTRACT

DNA polymerase  $\lambda$  (pol  $\lambda$ ) is a member of the X family DNA polymerases and is endowed with multiple enzymatic activities. In this work we investigated the *in vitro* miscoding properties of full-length, human pol  $\lambda$  either in the absence or in the presence of the human auxiliary proteins proliferating cell nuclear antigen (PCNA) and replication protein A (RP-A). Our data suggested that (i) pol  $\lambda$  had an intrinsic ability to create mismatches and to incorporate ribonucleotides at nearly physiological  $Mn^{++}$  and  $Mg^{++}$  concentrations; (ii) the sequence of the template-primer could influence the misincorporation frequency of pol  $\lambda$ ; (iii) pol  $\lambda$  preferentially generated G:T and G:G mismatches; (iv) RP-A, but not PCNA, selectively prevented misincorporation of an incorrect nucleotide by pol  $\lambda$ , without affecting correct incorporation and (v) this inhibitory effect required a precise ratio between the concentrations of pol  $\lambda$  and RP-A. Possible physiological implications of these findings for the *in vivo* fidelity of pol  $\lambda$  are discussed.

## INTRODUCTION

DNA polymerase  $\lambda$  (pol  $\lambda$ ) is a member of the pol family X, together with pol  $\beta$ , pol  $\mu$  and terminal deoxynucleotidyl transferase (TDT) (1). Pol  $\lambda$  is endowed with both template-dependent and template-independent (i.e. terminal transferase) DNA polymerase activities, as well as deoxyribose-5' phosphate lyase (dRPlyase) activity, suggesting multiple cellular roles for the enzyme (2,3). Indeed, the gene encoding pol  $\lambda$  was shown to be expressed at high level in the developing mouse testis (2) indicating a possible function

of pol  $\lambda$  in DNA synthesis associated with meiosis. Furthermore, it has been reported that proliferating cell nuclear antigen (PCNA) interacts with pol  $\lambda$ , increasing both its processivity during DNA synthesis and its ability to bypass an abasic site (4,5). These results suggest that pol  $\lambda$  may be involved in a PCNA-dependent DNA translesion synthesis pathway. Finally, both *in vitro* reconstitution of non-homologous end joining (NHEJ) process with purified proteins and immunodepletion studies with human nuclear extracts point to a role of pol  $\lambda$  in repair of double strand DNA breaks (DSBs) (6–8). Pol  $\lambda$  shares 33% sequence identity with pol  $\beta$  (3,9,10). Sequence alignment and three-dimensional structural determination showed that pol  $\lambda$  core contains the four conserved subdomains present in pol  $\beta$ . Unlike pol  $\beta$ , the N-terminal 132 amino acid residues of pol  $\lambda$  contain a nuclear localization signal motif and a BRCT domain. The template-dependent polymerase activity of pol  $\lambda$  has some distinct features compared with the one of pol  $\beta$ . In particular, pol  $\lambda$  appears to have evolved towards having an absolute preference for  $Mn^{++}$  as the metal activator, its catalytic activity being reduced at  $Mg^{++}$  concentrations higher than 2–3 mM (11). Thus, even though  $Mg^{++}$  is generally considered to be the physiological metal cofactor for pols, these results might suggest that pol  $\lambda$  *in vivo* is a  $Mn^{++}$ -dependent enzyme. The preference for either the  $Mg^{++}$  or  $Mn^{++}$  metal ion can have a great influence on the fidelity of DNA synthesis by a particular pol. Indeed, the high mutagenic potential of  $Mn^{++}$  as metal cofactor for DNA synthesis has been extensively shown. In an M13mp2 forward and reversion system (12), the fidelity of pol  $\lambda$  was estimated to be  $1.3\text{--}9.0 \times 10^{-4}$ . Pre-steady-state kinetic analysis of all possible misincorporations by a truncated form of pol  $\lambda$ , lacking the BRCT domain, showed that, in the presence of  $Mg^{++}$ , pol  $\lambda$  had even lower fidelities, ranging between  $10^{-2}$  and  $10^{-4}$ , depending on the particular basepair (13). Similar studies conducted with pol  $\beta$  and pol  $\mu$  showed fidelity values between  $10^{-3}$  and  $10^{-5}$  for both enzymes

\*To whom correspondence should be addressed at via Abbiategrasso 207, I-27100 Pavia, Italy. Tel: +39 038 254 6354; Fax: +39 038 242 2286; E-mail: maga@igm.cnr.it

(14,15). Thus, it appears that pol  $\lambda$  is the most error prone enzyme within the pol X family. Accordingly, overall base substitution rates for pol  $\lambda$  were shown to be 4-fold higher than for pol  $\beta$  in a forward mutation assay (16). However, pol  $\lambda$  was also shown to generate single base deletions at average rates substantially higher than its base substitution rates (16). This correlated with a remarkable tendency to create frequent primer/template misalignments, in the presence of micro-homology between the primer and template sequences (17).

PCNA and replication protein A (RP-A) are essential components of the cellular DNA replication and DNA repair machineries and have been shown to influence the enzymatic activities of pol  $\lambda$  (4,18). Therefore, it would be important to assess whether these two proteins could modulate the intrinsic miscoding ability of pol  $\lambda$ . To this aim, we have first characterized in detail the miscoding properties of full-length pol  $\lambda$  as a function of enzyme concentration, nucleotide concentration, divalent cations ( $Mn^{++}$  or  $Mg^{++}$ ) and DNA sequence context. Then, we measured the effect of PCNA and RP-A on such reactions. Our data suggest that RP-A but not PCNA could suppress the misincorporation ability of pol  $\lambda$ .

## MATERIALS AND METHODS

### Chemicals

[ $\gamma$ - $^{32}P$ ]ATP (3000 Ci/mmol) was from GE Healthcare Biosciences; unlabeled dNTPs, rNTPs, poly(dA)<sub>200</sub> and oligo(dT)<sub>16</sub>, were from Roche Molecular Biochemicals. All other reagents were of analytical grade and were purchased from Merck or Fluka.

### Nucleic acids substrates

All oligonucleotides were purified from polyacrylamide denaturing gels. The sequences are 17/75mer, 3'-ATAGG-TGGTATGATGGGAGGTGATAGAGGTGAGTTGAG-TTGGGAAGTAGGAAAGTTATAAGGATGGGAGGGCT-AG-5'; 18/40merA, 3'-ATAGGTGGTTATGATGGGATGC-TATGATAGAGGTGAGTTG-5'; 19/40merT, 3'-ATAGGT-GGTTATGATGGGATGCTATGATAGAGGTGAGTTG-5'; 20/40merG, 3'-ATAGGTGGTTATGATGGGATGCTATGATAGAGGTGAGTTG-5'; 21/40merC, 3'-ATAGGTGGTTA-TGATGGGATGCTATGATAGAGGTGAGTTG-5';

The sequence underlined corresponds to the primer hybridization position. In bold are the identical sequences shared among all five templates. The different primers were 5'-labelled with T4 polynucleotide kinase (New England Biolabs) in the presence of [ $\gamma$ - $^{32}P$ ]ATP. For the preparation of the corresponding primer/template substrates, each labelled primer was mixed to the complementary template oligonucleotide at 1:1 (M/M) ratio in the presence of 25 mM Tris-HCl pH 8.0 and 50 mM KCl, heated at 80°C for 3 min and then slowly cooled down at room temperature.

### Proteins production and purification

Recombinant His-tagged human wild-type pol  $\lambda$ , human PCNA and human RP-A were expressed and purified as described (19–21). After purification, the proteins were >90% homogenous, as judged by SDS-PAGE and Coomassie staining.

### Enzymatic assays

For denaturing gel analysis of pol  $\lambda$  DNA synthesis products, the reaction mixtures contained 50 mM Tris-HCl (pH 7.0), 0.25 mg/ml BSA, 1 mM DTT and 30 nM (0.3 pmol of 3' OH ends) of the different 5'  $^{32}P$ -labelled primer/ templates (unless otherwise stated). Concentrations of pols, PCNA, RP-A, dNTPs and either  $Mg^{++}$  or  $Mn^{++}$  were as indicated in the corresponding figure legends. Reactions were incubated 15 min at 37°C and then stopped by addition of standard denaturing gel loading buffer (95% formamide, xylene cyanol and bromophenol blue), heated at 95°C for 3 min and loaded on a 7 M urea/15% polyacrylamide gel.

### Steady state kinetic analysis

Reactions were performed in the presence of 50 mM Tris-HCl (pH 7.0), 0.25 mg/ml BSA, 1 mM DTT, 50 nM (0.5 pmol of 3' OH ends) of the different 5'  $^{32}P$ -labelled primer/templates and either 0.1 mM  $Mn^{++}$  or 1 mM  $Mg^{++}$ . For correct nucleotide incorporation, 8 nM pol  $\lambda$  (corresponding to 0.08 pmol) were used, whereas for incorrect nucleotide incorporation, the enzyme concentration was raised to 25 nM (0.25 pmol). Conditions for incorrect nucleotides incorporation were determined in a set of preliminary experiments aimed at establishing the best approximating steady-state conditions still allowing the detection of mismatched products. Reactions were incubated for 10 min, which was the midpoint of the linear range of the reaction, as determined in preliminary experiments. Nucleotide concentrations used ranged from 0.1 to 10  $\mu$ M. Under all conditions, the amount of elongated primers were always <20–25% of the input. Maximum nucleotide substrate utilization was <10% of the input. Quantification was done by scanning densitometry. The initial velocities of the reaction were calculated from the values of integrated gel band intensities:

$$I^*_T/I_{T-1},$$

where T is the target site, the template position of interest;  $I^*_T$  = the sum of the integrated intensities at positions T, T + 1, ..., T + n.

All the intensity values were normalized to the total intensity of the corresponding lane to correct for differences in gel loading. An empty lane was scanned and the corresponding value subtracted as background. The apparent  $K_d$  and  $k_{cat}$  values were calculated by plotting the initial velocities in dependence of the substrate concentrations and fitting the data according to the Michaelis-Menten equation in the form

$$v = k_{cat}[E]_0/(1 + K_d/[S]),$$

where  $[E]_0$  was the input enzyme concentration.

Nucleotide incorporation efficiencies were defined as the  $k_{cat}/K_d$  ratio. Frequencies of misincorporations ( $f_{mis}$ ) were calculated as the ratio between the  $k_{cat}/K_d$  values for correct and incorrect nucleotides. Under single nucleotide incorporation conditions  $k_{cat} = k_{pol}k_{off}/(k_{pol} + k_{off})$  and  $K_d = K_s k_{off}/(k_{pol} + k_{off})$ , where  $k_{pol}$  is the true polymerization rate,  $k_{off}$  is the dissociation rate of the enzyme-primer complex and  $K_s$  is the true Michaelis constant for nucleotide binding. Thus,  $k_{cat}/K_d$  values are equal to  $k_{pol}/K_s$ . Fidelity, i.e. the number of correct incorporation events before a mismatch occurs, was expressed as  $1/f_{mis}$ .

## RESULTS

### DNA polymerase $\lambda$ can misincorporate deoxyribonucleotides in the presence of nearly physiological $Mn^{++}$ and $Mg^{++}$ concentrations

$Mn^{++}$  is an essential cofactor for many enzymes. It can be accumulated intracellularly by specific import pathways, e.g. in liver and brain, reaching concentrations of 0.05–0.1 mM (22). Since pol  $\lambda$  was shown to be particularly active over a wide range of  $Mn^{++}$  concentration (11), we first tested all four possible dNTPs combinations in the presence of each templating base (A, T, G, C) at a nearly physiological  $Mn^{++}$  concentration of 0.1 mM (Figure 1A). Six mismatches (X:Y, where X is the incoming dNTP and Y is the templating base) were detected, namely C:A, G:T, C:T, T:G, G:G and A:C (Figure 1A, lanes 3, 8, 9, 12, 13 and 16, respectively). The same experiments were repeated in the presence of 1 mM  $Mg^{++}$ . Owing to the known inhibitory effect of high  $Mg^{++}$  concentrations on pol  $\lambda$  (11), 1 mM  $Mg^{++}$  concentration was used since it lies within the physiological  $Mg^{++}$  concentration range and is still compatible with significant pol  $\lambda$  activity. As shown in Figure 1B, only three mismatches were generated: G:T, C:T and G:G (Figure 1B, lanes 8, 9 and 14, respectively). Thus,  $Mg^{++}$  reduced, but did not abolish, the ability of pol  $\lambda$  to misincorporate nucleotides. These results suggest that pol  $\lambda$  is able to make mismatches in the presence of both  $Mn^{++}$  and  $Mg^{++}$ .

### DNA polymerase $\lambda$ is able to incorporate ribonucleotides

Pol  $\beta$  and  $\mu$ , both closely related to pol  $\lambda$ , have a low discrimination capacity between ribo- and deoxynucleotides (23,24). In order to investigate whether pol  $\lambda$  was able to incorporate ribonucleotides (rNTPs) on a DNA template, all four rNTPs were tested in the presence of each templating base at nearly physiological concentrations of either  $Mn^{++}$  or  $Mg^{++}$ . In the presence of  $Mn^{++}$ , all the four correctly base-paired rNTPs were incorporated (Figure 1C, lanes 2, 5, 14 and 19, respectively), with synthesis of short RNAs in the presence of a mixture of all four rNTPs (lanes 9 and 15). Incorporation of correctly base-paired rNTPs was also observed in the presence of  $Mg^{++}$ , in the case of A, C and G (lanes 25, 33 and 38, respectively), but not U (lane 22). However, subsequent experiments showed that pol  $\lambda$  was able to incorporate also UTP under similar conditions but on different sequence contexts (see below). It should be noted that misincorporation of rCTP was detected with the 19/40merT template in the presence of  $Mn^{++}$  (lane 8). Inspection of the sequence revealed that the templating base at position +2 was G. Thus, this incorporation is likely due to primer/template slippage, with the base at position +2 used as a template. This is consistent with the known ability of pol  $\lambda$  to generate frequent slippage (16). In summary, these results demonstrate that pol  $\lambda$  is able to incorporate rNTPs under nearly physiological  $Mn^{++}$  and  $Mg^{++}$  concentrations.

### Misincorporation by DNA polymerase $\lambda$ is influenced by the template sequence context

Next, we tested the level of misincorporation of pol  $\lambda$  when replicating DNA templates with different sequence context. Results are shown in Figure 2A with a 17/75mer template,

where the sequence of the first six template positions is AGGTGA, instead of the ATGCTA sequence present in the 18/40mer template previously used (Figure 1). On this substrate all possible mismatches were detectable in the presence of  $Mn^{++}$  (lanes 1–4), and, under these conditions, pol  $\lambda$  also generated all four mismatches in the presence of rNTPs (lanes 6–9). When compared with similar reactions performed with the 18/40mer template (Figure 1A–C), whose initial templating sequence contains a reduced number of purine residues, an increase in the misincorporation ability of pol  $\lambda$  can be observed and some products longer than 1 nt accumulated. In the case of dCTP and CTP (Figure 2A, lanes 3 and 8, respectively), these products are likely due to template-slippage, with the two G residues at position +2/+3 acting as templating bases (17), while, in the case of dTTP and UTP (lanes 4 and 9, respectively) the long products are likely to be the result of misincorporations. In the presence of  $Mg^{++}$  (Figure 2B), a significant increase in misincorporation of pol  $\lambda$  was also noted in comparison with the experiments shown in Figure 1B. However, all the misincorporations generated exclusively +1 products. One possible explanation for this finding could be the reported increase in pol  $\lambda$  distributivity in presence of  $Mg^{++}$  compared with  $Mn^{++}$  (11). Results in Figure 2A and B suggested that the misincorporation capacity of pol  $\lambda$  is enhanced during replication of a purine-rich tract of DNA. To investigate further on this possibility, the fidelity of pol  $\lambda$  was examined with homopolymeric polypurinic primer/template (dT)<sub>16</sub> / (dA)<sub>200</sub>. Figure 2C shows that A:A, G:A and C:A mismatches were detectable by measuring misincorporation of deoxyribonucleosides. In addition, consecutive mismatches could be detected (lanes 3 and 4, respectively). With rNTPs, pol  $\lambda$  generated G:A and C:A mismatches (lanes 8 and 9, respectively), and in the presence of the correctly matched UTP, pol  $\lambda$  synthesised short (3–4 nt) RNAs (lane 7). Replacement of  $Mn^{++}$  with  $Mg^{++}$  prevented misincorporation of rNTPs, allowing the incorporation of the correctly matched UTP and solely up to +1 product (Figure 2D, lane 7), but did not significantly influence the misincorporation of dNTPs (Figure 2D, lanes 2–4). These data suggested that on polypurinic sequences,  $Mg^{++}$  can substantially increase ribo- versus deoxy- discrimination with respect to  $Mn^{++}$ , but not the base-pairing fidelity.

To investigate further the increased capacity of pol  $\lambda$  to misincorporate when replicating a purine-rich template, we compared the apparent binding affinities of all four dNTPs with the enzyme when acting on the homopolymeric polypurinic primer/template (dT)<sub>16</sub> / (dA)<sub>200</sub> or on the homopolymeric polypyrimidinic primer/template (dA)<sub>16</sub> / (dT)<sub>200</sub> in the presence of 1 mM  $Mg^{++}$  (Table 1). Both correct and incorrect nucleotides were able to bind to pol  $\lambda$  with higher affinities with the polypurinic template than with the polypyrimidinic one. In addition, the apparent rates of incorporation ( $k_{cat}$ ) were lower for mismatched nucleotides on the polypyrimidinic template, with respect to the polypurinic one. Replacement of  $Mg^{++}$  with  $Mn^{++}$  gave similar results, but the affinities of the incorrect nucleotides were higher than in the presence of  $Mg^{++}$  (data not shown). Taken together, these results showed that pol  $\lambda$  can synthesise DNA with decreased fidelity when challenged with polypurine tracts and this even in the presence of  $Mg^{++}$ .

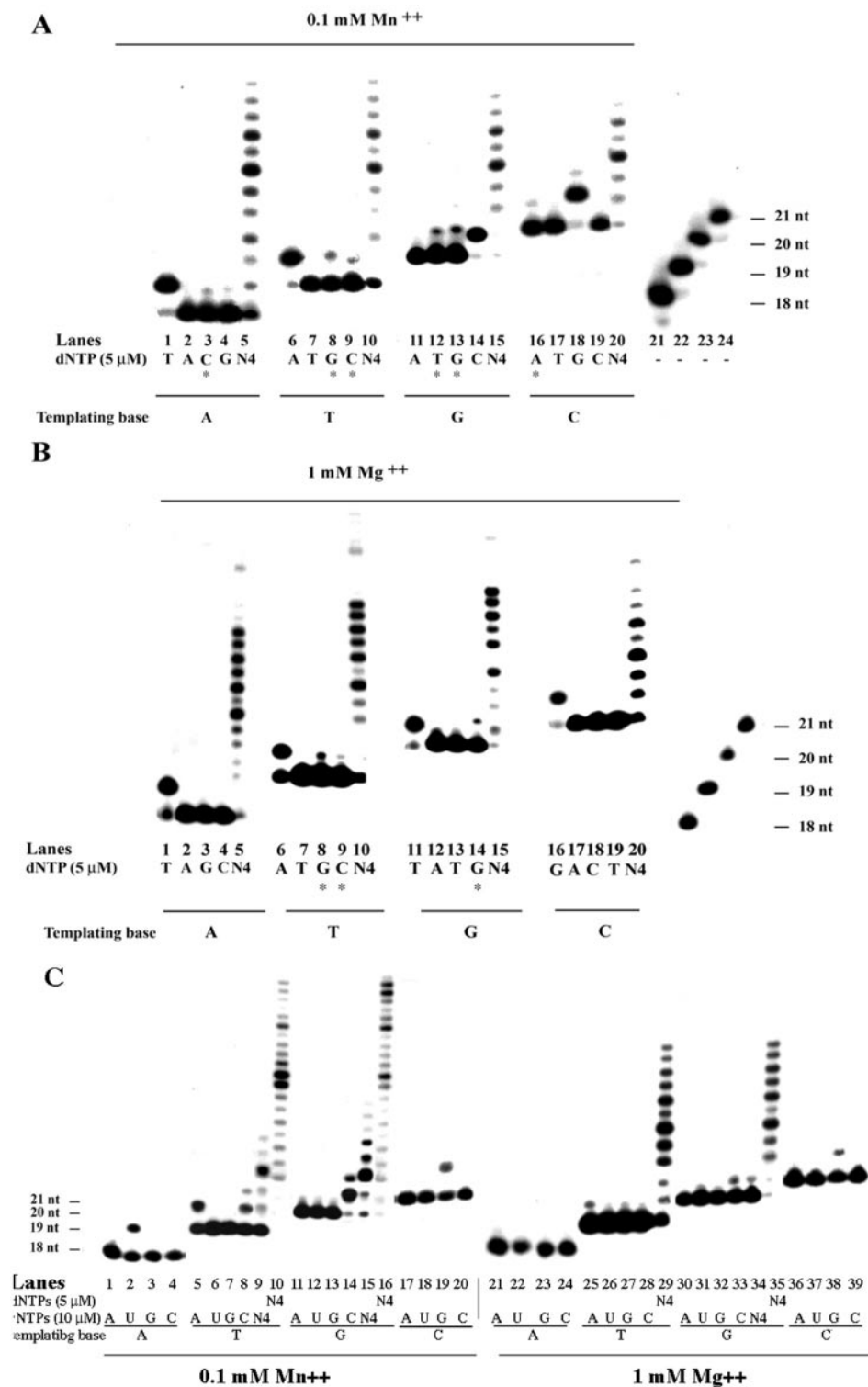


**Figure 1.** Pol  $\lambda$  can misincorporate deoxy- and ribonucleotides in the presence of physiological Mn<sup>++</sup> and Mg<sup>++</sup> concentrations. The sequences of the primer/ templates used are indicated in Materials and Methods. (A) Reactions were performed as described in Materials and Methods, in the presence of 50 nM (0.5 pmol) pol  $\lambda$ , 0.1 mM Mn<sup>++</sup> and each of the four dNTPs at 5  $\mu$ M final concentration. Lanes 1–4: 5'-labelled 18/40merA primer/template; lanes 6–9: 19/40merT; lanes 11–14: 20/40merG; lanes 16–19: 21/40merC. Lanes 5, 10, 15 and 20: control reactions with all four dNTPs at 5  $\mu$ M each. Lanes 21–24: control reactions in the absence of dNTPs. Asterisks indicate the mismatches. (B) The experiment was performed as in panel A, but in the presence of 1 mM Mg<sup>++</sup>. The migration of four different primers is shown on the right side of the panel. Asterisks indicate the mismatches. (C) Reactions were performed as described in Materials and Methods in the presence of 50 nM (0.5 pmol) pol  $\lambda$ , 0.1 mM Mn<sup>++</sup> (lanes 1–20) or 1 mM Mg<sup>++</sup> (lanes 21–39) and each of the four rNTPs at a final concentration of 10  $\mu$ M. Lanes 1–4; 21–24: 5'-labelled 18/40merA primer/template; lanes 17–20; 25–28: 19/40merT; lanes 11–15, 30–33: 20/40merG; lanes 16–19; 36–39: 21/40merC. Lanes 9, 15 and 34: reactions in the presence of a mixture of all four rNTPs at 10  $\mu$ M each. Lanes 10, 16, 29 and 35: control reactions in the presence of all four dNTPs at 5  $\mu$ M each final concentration. The running position of the four different primers is indicated on the left side of the panel.

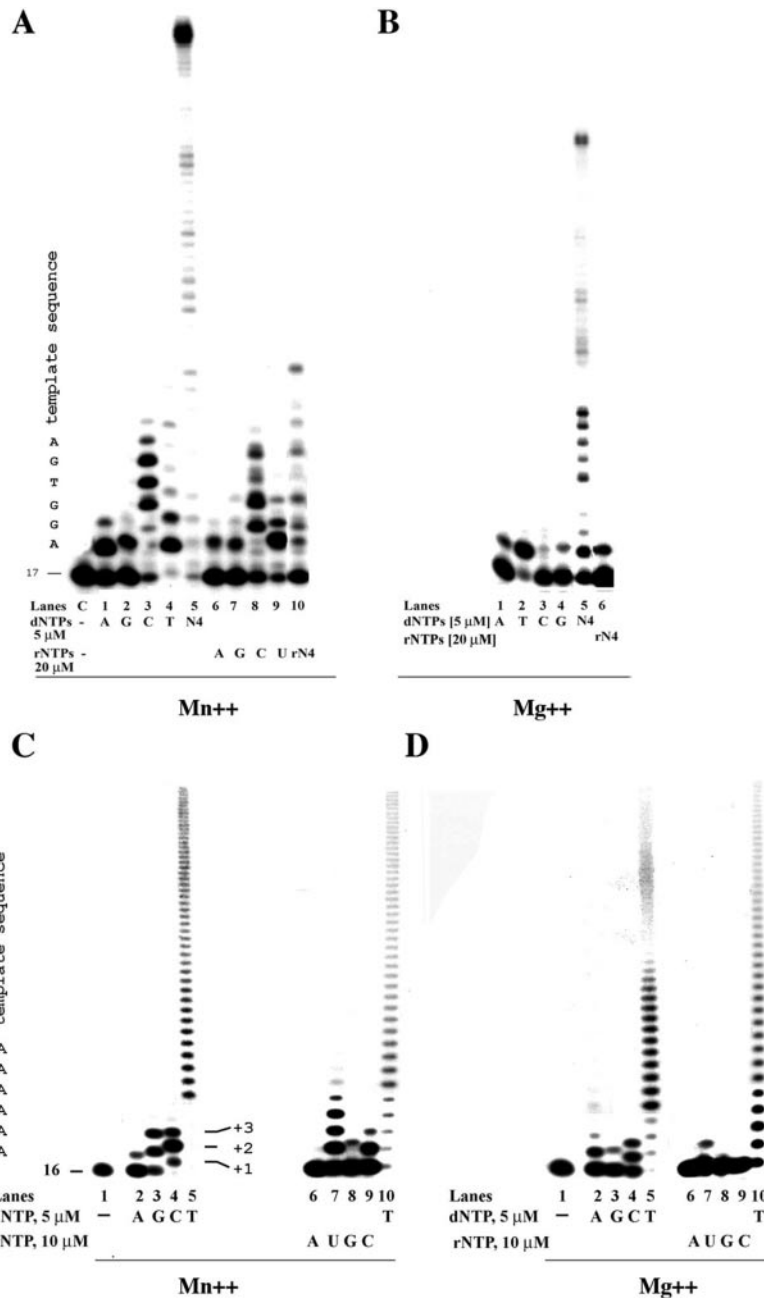


**Figure 2.** The sequence context influences misincorporation by pol  $\lambda$ . All reactions were performed as described in Materials and Methods in the presence of 50 nM (0.5 pmol) pol  $\lambda$ . (A) Incorporation of the four dNTPs (lanes 1–4, 5  $\mu$ M final concentration) or the four rNTPs (lanes 6–9, 20  $\mu$ M final concentration) on the 5'-labelled 17/75mer primer template, in the presence of 0.1 mM  $Mn^{++}$ . Lane C: control reaction in the absence of dNTPs or rNTPs. Lane 5: reaction in the presence of all four dNTPs (5  $\mu$ M each). Lane 10: reaction in the presence of all four rNTPs (20  $\mu$ M each). The position of the 17mer primer and the sequence of the first six positions on the template strand are indicated on the left side of the panel. (B) Reaction conditions were the same as for panel A, but 1 mM  $Mg^{++}$  was used instead of  $Mn^{++}$ . The four dNTPs were added individually (lanes 1–4) or all together (lane 5) at a final concentration of 5  $\mu$ M each. Lane 6: reaction in the presence of all four rNTPs at 20  $\mu$ M final concentration each. (C) Reaction conditions were as in panel A, but the 5'-labelled d(T)<sub>16</sub>/d(A)<sub>200</sub> primer/template was used. All four dNTPs (lanes 2–5) or rNTPs (lanes 6–9) were tested separately at a final concentration of 5  $\mu$ M for dNTPs and 10  $\mu$ M for rNTPs, in the presence of 0.1 mM  $Mn^{++}$ . (D) Reaction conditions were the same as C, but 1 mM  $Mg^{++}$  was used instead of  $Mn^{++}$ .

### DNA polymerase $\lambda$ preferentially generates G:T and G:G mismatches

Next we focused on the three deoxyribonucleotide mismatches G:T, C:T and G:G, that we detected in the presence of both  $Mn^{++}$  and  $Mg^{++}$  since they may represent the most probable mutagenic events *in vivo*. First we established that, in the

case of G:T and C:T and in the presence of 0.1 mM  $Mn^{++}$ , the efficiency of mismatch formation was dependent on both the enzyme (Figure 3A) and the nucleotide (Figure 3B) concentrations, with a preference for the formation of G:T over the C:T mismatch. The kinetic parameters for correct versus incorrect incorporation by pol  $\lambda$  were determined in the presence of both  $Mn^{++}$  and  $Mg^{++}$ , and the calculated values are

**Table 1.** Kinetic constants for dNTPs incorporation by pol  $\lambda$  on (dT)<sub>16</sub>/d(A)<sub>200</sub> and d(A)<sub>16</sub>/(dT)<sub>200</sub>

Templating base	Incoming dNTP	$K_d$ , $\mu\text{M}$	$k_{\text{cat}}$ , $\text{min}^{-1}$	$K_d$ , $\mu\text{M}$ + RP-A <sup>a</sup>	$k_{\text{cat}}$ , $\text{min}^{-1}$ + RP-A
A	<b><i>dTTP</i></b>	<b><i>1.2 (<math>\pm 0.1</math>)</i></b>	0.2 ( $\pm 0.02$ )	<b><i>1 (<math>\pm 0.1</math>)</i></b>	0.55 ( $\pm 0.03$ )
	dGTP	2.3 ( $\pm 0.3$ )	0.02 ( $\pm 0.002$ )	9.9 ( $\pm 0.8$ )	0.01 ( $\pm 0.002$ )
	dCTP	2.8 ( $\pm 0.4$ )	0.04 ( $\pm 0.005$ )	10 ( $\pm 1$ )	0.03 ( $\pm 0.005$ )
	dATP	2.2 ( $\pm 0.2$ )	0.075 ( $\pm 0.007$ )	12 ( $\pm 1$ )	0.055 ( $\pm 0.007$ )
T	<b><i>dATP</i></b>	<b><i>1 (<math>\pm 0.1</math>)</i></b>	0.15 ( $\pm 0.02$ )	<b><i>1 (<math>\pm 0.1</math>)</i></b>	0.45 ( $\pm 0.02$ )
	dGTP	7.5 ( $\pm 0.5$ )	0.005 ( $\pm 0.001$ )	37 ( $\pm 4$ )	0.004 ( $\pm 0.001$ )
	dCTP	10 ( $\pm 1$ )	0.02 ( $\pm 0.001$ )	40 ( $\pm 3$ )	0.01 ( $\pm 0.001$ )
	dTTP	13 ( $\pm 1$ )	0.025 ( $\pm 0.002$ )	53 ( $\pm 5$ )	0.015 ( $\pm 0.002$ )

RP-A concentrations used were 0.025, 0.05, 0.1, 0.25 and 0.5 pmol, respectively. Numbers in brackets are  $\pm$ S.D. from three independent experiments.

<sup>a</sup> $K_d$  was calculated by analyzing the variation of the apparent affinity [ $K_d(\text{app})$ ] of pol  $\lambda$  for the different dNTPs as a function of [RP-A] concentration, according to the equation  $K_d(\text{app}) = K_d / (1 + K_s / [\text{RP-A}])$ , where  $K_s$  is the apparent dissociation constant of the [RP-A: DNA:pol  $\lambda$ ] complex. 1 mM  $\text{Mg}^{++}$  was used in all the reactions. Pol  $\lambda$  was used at 50 nM (0.5 pmol) final concentration.

The apparent affinity for correct nucleotide incorporation on both templates is highlighted (bold italic)

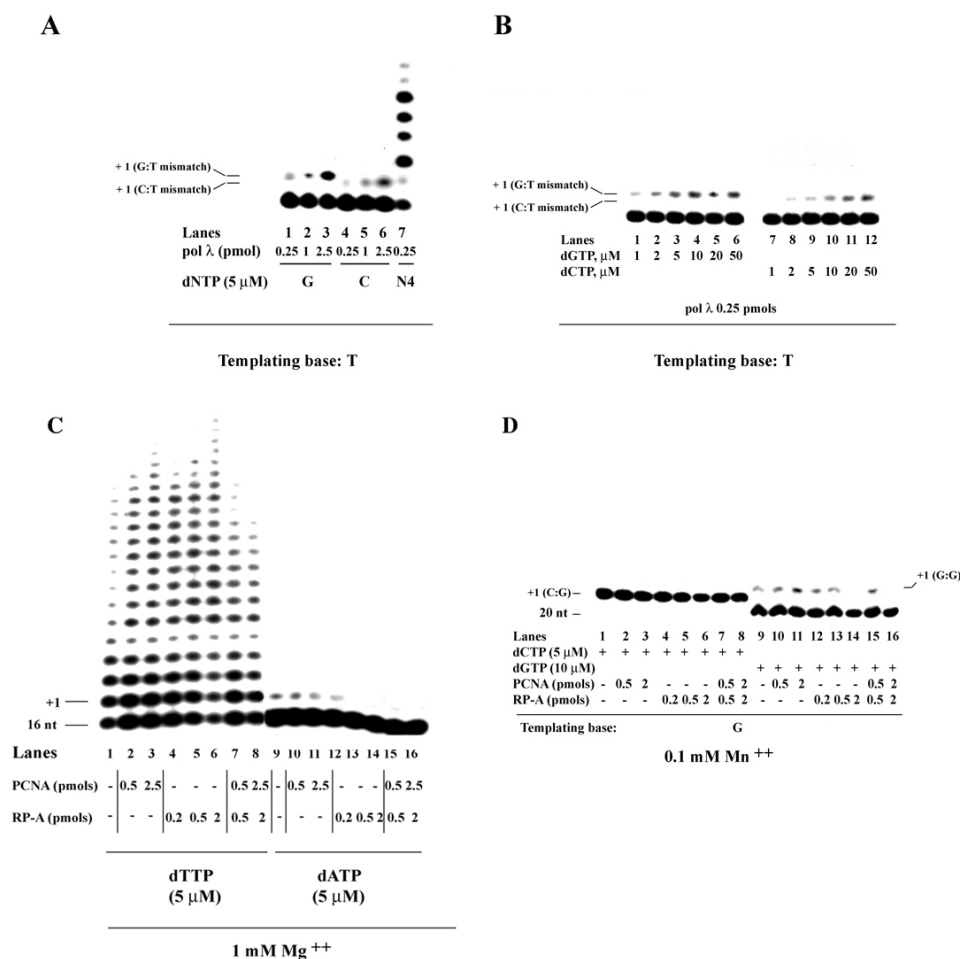


**Figure 3.** Pol  $\lambda$  appears to preferentially generate G:T over C:T mismatches and its misincorporation ability is suppressed by RP-A. (A) Misincorporation of dGTP (lanes 1–3) or dCTP (lanes 4–6) was monitored on the 19/40merT template in the presence of 0.1 mM  $\text{Mn}^{++}$  and increasing concentrations of pol  $\lambda$  (25, 100 and 250, corresponding to 0.25, 1 and 2.5 pmol, respectively). Lane 7: control reaction in the presence of 25 nM pol  $\lambda$  and all four dNTPs at 5  $\mu\text{M}$  each. The positions of the differently migrating dGMP- and dCMP-terminated +1 products are shown on the left side of the panel. (B) Misincorporation of increasing concentrations of dGTP (lanes 1–6) or dCTP (lanes 7–12) were monitored on the 19/40merT template in the presence of 0.1 mM  $\text{Mn}^{++}$  and 25 nM (0.25 pmol) pol  $\lambda$ . The positions of the differently migrating dGMP- and dCMP-terminated +1 products are shown on the left side of the panel. (C) Incorporation of dTTP or dATP (5  $\mu\text{M}$  each) was measured in the presence of 50 nM (0.5 pmol) pol  $\lambda$ , 5'-labelled d(T)<sub>16</sub>/d(A)<sub>200</sub> primer/template, 1 mM  $\text{Mg}^{++}$  and in the absence (lanes 1 and 9) or in the presence of different concentrations of either PCNA (lanes 2, 3, 10 and 11) or RP-A (lanes 4–6, 12–14), or an equimolar combination of both proteins (lanes 7, 8, 15 and 16). (D) Incorporation of 5  $\mu\text{M}$  dCTP (lanes 1–8) or 10  $\mu\text{M}$  dGTP (lanes 9–16) was monitored on the 5'-labelled 20/40merG primer/template, in the presence 150 nM (1.5 pmol) pol  $\lambda$ , 0.1 mM  $\text{Mn}^{++}$ , and in the absence (lanes 1 and 9) or in the presence of 0.5 (lanes 2, 10) and 2 pmol (lanes 3, 11) of PCNA, or 0.2 (lanes 4, 12), 0.5 (lanes 5, 13) and 2 pmol (lanes 6, 14) of RP-A, or a combination of 0.2 (lanes 7, 15) or 2 pmol (lanes 15, 16) of PCNA and RP-A in equimolar ratios. The positions of the differently migrating dCMP- and dGMP-terminated primers are indicated on the left side of the panel with an asterisk.

**Table 2.** Kinetic parameters for correct and incorrect nucleotide incorporation by pol  $\lambda$ 

Template/Primer	Incoming nucleotide	0.1 mM Mn <sup>++</sup>				1 mM Mg <sup>++</sup>			
		K <sub>d</sub> $\mu$ M	k <sub>cat</sub> min <sup>-1</sup>	k <sub>cat</sub> /K <sub>d</sub> $\mu$ M <sup>-1</sup> min <sup>-1</sup>	Fidelity 1/f <sub>inc</sub>	K <sub>d</sub> $\mu$ M	k <sub>cat</sub> min <sup>-1</sup>	k <sub>cat</sub> /K <sub>d</sub> $\mu$ M <sup>-1</sup> min <sup>-1</sup>	Fidelity 1/f <sub>inc</sub>
18/40merA	dTTP	1.5 <sup>a</sup> ( $\pm$ 0.1)	0.2 ( $\pm$ 0.02)	0.13 ( $\pm$ 0.01)	1	n.d. <sup>b</sup>	n.d.	n.d.	n.d.
	UTP	4.5 ( $\pm$ 0.8)	0.02 ( $\pm$ 0.05)	0.004 ( $\pm$ 0.001)	32.5	n.d.	n.d.	n.d.	n.d.
19/40merT	dATP	1.2 ( $\pm$ 0.1)	0.12 ( $\pm$ 0.02)	0.1 ( $\pm$ 0.05)	1	0.8 ( $\pm$ 0.1)	0.05 ( $\pm$ 0.01)	0.0625 ( $\pm$ 0.01)	1
	dCTP	4.5 ( $\pm$ 0.5)	0.01 ( $\pm$ 0.003)	0.0022 ( $\pm$ 0.0002)	45	4.5 ( $\pm$ 0.5)	0.002 ( $\pm$ 0.0005)	0.0004 ( $\pm$ 0.0001)	156
	dGTP	2.5 ( $\pm$ 0.2)	0.02 ( $\pm$ 0.01)	0.008 ( $\pm$ 0.01)	12.5	3 ( $\pm$ 0.3)	0.008 ( $\pm$ 0.004)	0.002 ( $\pm$ 0.0003)	31
	ATP	3.7 ( $\pm$ 2)	0.015 ( $\pm$ 0.005)	0.004 ( $\pm$ 0.001)	25	12 ( $\pm$ 2)	0.01 ( $\pm$ 0.002)	0.0008 ( $\pm$ 0.0001)	187
20/40merG	dCTP	1.5 ( $\pm$ 0.1)	0.5 ( $\pm$ 0.2)	0.33 ( $\pm$ 0.04)	1	0.9 ( $\pm$ 0.1)	0.2 ( $\pm$ 0.08)	0.22 ( $\pm$ 0.03)	1
	dGTP	1.4 ( $\pm$ 0.1)	0.04 ( $\pm$ 0.003)	0.028 ( $\pm$ 0.006)	11.7	0.8 ( $\pm$ 0.2)	0.004 ( $\pm$ 0.001)	0.005 ( $\pm$ 0.001)	44
	CTP	2.7 ( $\pm$ 0.5)	0.08 ( $\pm$ 0.01)	0.029 ( $\pm$ 0.004)	26.5	9 ( $\pm$ 2)	0.01 ( $\pm$ 0.003)	0.0011 ( $\pm$ 0.0002)	220
21/40merC	dGTP	2.5 ( $\pm$ 0.2)	0.2 ( $\pm$ 0.03)	0.08 ( $\pm$ 0.02)	1	3 ( $\pm$ 0.4)	0.08 ( $\pm$ 0.01)	0.026 ( $\pm$ 0.002)	1
	GTP	6.5 ( $\pm$ 0.7)	0.03 ( $\pm$ 0.01)	0.0075 ( $\pm$ 0.001)	17	10 ( $\pm$ 1)	0.003 ( $\pm$ 0.001)	0.0003 ( $\pm$ 0.0001)	87
d(T) <sub>16</sub> /d(A) <sub>200</sub>	dTTP	n.d.	n.d.	n.d.	n.d.	1.2 ( $\pm$ 0.2)	0.2 ( $\pm$ 0.03)	0.17 ( $\pm$ 0.07)	1
	dATP	n.d.	n.d.	n.d.	n.d.	2.2 ( $\pm$ 0.2)	0.075 ( $\pm$ 0.007)	0.034 ( $\pm$ 0.006)	5
	dCTP	n.d.	n.d.	n.d.	n.d.	2.8 ( $\pm$ 0.4)	0.04 ( $\pm$ 0.005)	0.014 ( $\pm$ 0.002)	12
	dGTP	n.d.	n.d.	n.d.	n.d.	2.3 ( $\pm$ 0.3)	0.02 ( $\pm$ 0.002)	0.008 ( $\pm$ 0.002)	21

<sup>a</sup>Values are the means of three independent experiments. Numbers in parenthesis are  $\pm$  SD. Reactions conditions and kinetic parameters calculations were as described in Materials and Methods

<sup>b</sup>not determined.

shown in Table 2. Even though one has to be cautious when interpreting steady-state kinetic data for nucleotide incorporation, since the steady-state K<sub>d</sub> and k<sub>cat</sub> values are a combination of different rates, our data, within the limit of multiple turnover kinetic measurements, allowed the following observations. First, Mg<sup>++</sup> increased the fidelity of pol  $\lambda$  by 4–8 times in the case of dNTPs and 9–20 times in the case of rNTPs. Second, the lowest fidelity values were those for the G:T and G:G mismatches, respectively, in the presence of both metal cofactors. In particular, the fidelity value for G:T mismatch generation in the presence of Mg<sup>++</sup> was 31, compared with the 156 value for the C:T mismatch.

Mismatch generation was also investigated in the presence of Mg<sup>++</sup> with the d(T)<sub>16</sub>/d(A)<sub>200</sub> substrate. As seen in Table 2, fidelity values for A:A and C:A mismatches on this template were 5 and 12, respectively. We also noted that the corresponding mismatches were so unfavoured with the 18/40mer template that they could not be detected at this enzyme concentration, even in the presence of Mn<sup>++</sup>.

### Replication protein A can enhance the fidelity of DNA polymerase $\lambda$

The results presented so far showed that *in vitro* synthesis by pol  $\lambda$  is potentially mutagenic in the presence of both Mn<sup>++</sup> and Mg<sup>++</sup>. Since it has been shown that pol  $\lambda$  functionally interacts with the auxiliary proteins PCNA and RP-A (4,18), we tested whether PCNA and RP-A can affect the misincorporation ability of pol  $\lambda$  on the (dT)<sub>16</sub>/ (dA)<sub>200</sub> substrate. The choice of this template was attributed to the fact that pol  $\lambda$  displayed a strong mutator phenotype on this template (Figure 2). As shown in Figure 3C, lane 9, pol  $\lambda$  was able to generate an A:A mismatch in the presence of Mg<sup>++</sup>. Addition of PCNA under these conditions did not prevent the misincorporation (lanes 10, 11) However, addition of RP-A, either in the absence or in the presence of PCNA (lanes 13 and 14 and lanes 15 and 16, respectively), suppressed misincorporation by pol $\lambda$ . This effect was dose-dependent, with partial suppression at the lowest RP-A dose (0.2 pmol) and complete inhibition at higher concentrations. This dose-dependent effect was investigated further as detailed in the

next section. Therefore, RP-A appears to strongly reduce the misincorporation capacity of pol  $\lambda$ . Importantly, neither PCNA nor RP-A affected the incorporation of the correctly base-paired dTTP (lanes 1–8). Figure 3D shows the effect of RP-A on the incorporation of dCTP and on the misincorporation of dGTP with another template (20/40merG) and in the presence of 0.1 mM Mn<sup>++</sup>. Incorporation of the correct nucleotide dCTP resulted in the complete elongation of the input substrate (lane 1). PCNA and RP-A either alone (lanes 2 and 3 and lanes 4–6, respectively) or in combination (lanes 7 and 8) did not affect correct nucleotide incorporation. Under these experimental conditions, the processivity of the reaction was restricted to a single nucleotide incorporation, suggesting that PCNA did not show any effect (17). When the incorrect dGTP was tested as the incoming nucleotide in place of dCTP, incorporation was, as expected, less efficient, but a mismatched product could be detected (lane 9). The different nature of the resulting dGMP-terminated product produced a shift in electrophoretic mobility compared with the correctly dCMP-terminated primer (compare lanes 1–8 with lanes 9–18). Addition of PCNA (lanes 10–11) did not reduce the misincorporation of dGTP. In striking contrast, addition of 2 pmol of RP-A either alone (lane 14) or in combination with equimolar amounts of PCNA (lane 16), completely prevented dGTP misincorporation. In summary, RP-A is able to specifically prevent incorrect nucleotide incorporation by pol  $\lambda$  in the absence as well as in the presence of PCNA.

### Suppression of pol $\lambda$ misincorporation ability by RP-A requires a precise balance between the concentration of the two proteins

In further experiments increasing amounts of RP-A were titrated into a reaction in the presence of different pol  $\lambda$  concentrations, and incorporations of either dATP (correct) or dGTP (mismatched) were monitored on the template 19/40mer T (Figure 4A). The data suggested the amount of RP-A required to achieve complete suppression of incorrect dGTP incorporation was directly proportional to the amount of pol  $\lambda$  and correlated with an almost equimolar RP-A: pol  $\lambda$

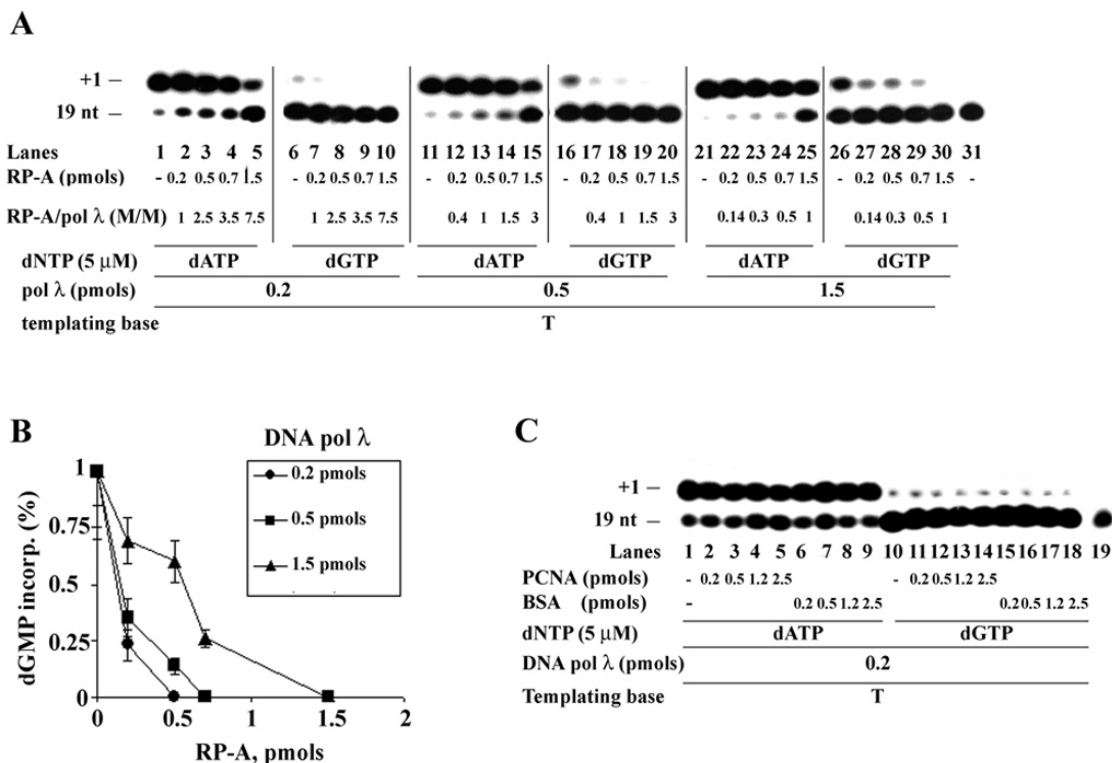


**Figure 4.** A precise balance of the relative concentrations of RP-A and pol λ is required for suppression of misincorporation. All reactions were performed as described in Materials and Methods in the presence of 0.1 mM  $Mn^{++}$  and the 5'-labelled 19/40merT template. (A) Incorporation of 5 μM dATP (lanes 1–5, 11–15, 21–25) or 5 μM dGTP (lanes 6–10, 16–20, 26–30), was monitored in the presence of 0.2 (lanes 1–10), 0.5 (lanes 11–20) and 1.5 pmol (lanes 21–30) of pol λ, corresponding to final enzyme concentrations of 20, 50 and 150 nM, respectively. Reactions were performed in the absence (lanes 1, 6, 11, 16, 21 and 26) or in the presence (lanes 2–5, 7–10, 12–15, 17–20, 22–25, 26–30) of increasing amounts of RP-A, as indicated in the panel. The resulting molar/molar (M/M) ratios of RP-A to pol λ in the different reactions are also indicated. (B) Misincorporated dGMP, in the absence or in the presence of RP-A, was quantified from the experiment shown in panel A. The normalized values, expressed as percentages of the total dGMP incorporated in the absence of RP-A in each set of reactions, were plotted as a function of the RP-A concentrations. Three different exposition times were used to collect images representative of the entire dynamic range of the X-ray film sensitivity. Images were scanned independently and the mean values of the three independent measurements were used for the plot. Error bars indicate  $\pm$  SD; circles, values calculated in the presence of 0.2 pmol (20 nM) DNA pol λ; squares, values calculated in the presence of 0.5 pmol (50 nM) DNA pol λ; triangles, values calculated in the presence of 1.5 pmol (150 nM) pol λ. The actual misincorporation values in the absence of RP-A (expressed as percentage elongation of the input DNA substrate) were 4.5 ( $\pm$ 0.5)% with 0.2 pmol pol λ, 15.8 ( $\pm$ 0.8)% with 0.5 pmol DNA pol λ and 37.5 ( $\pm$ 0.8)% with 1.5 pmol DNA pol λ. (C) As a control, incorporation of dATP (lanes 1–9) or dGTP (lanes 10–18) in the presence of 0.1 mM  $Mn^{++}$  and 0.2 pmol (20 nM) of pol λ was monitored in the absence (lanes 1 and 10) or in the presence of increasing amounts of PCNA (lanes 2–5, 11–14) or BSA (lanes 6–9, 15–18). Lane 19: control reaction in the absence of dNTPs.

ratio (compare lanes 7, 18 and 30). Products from the results depicted in Figure 4A were quantified and the percentage of residual dGMP misincorporation was plotted as a function of RP-A concentrations (Figure 4B). The concentrations of RP-A resulting in 50% inhibition of dGMP misincorporation by pol λ were 0.14 ( $\pm$ 0.01) pmol RP-A/0.2 pmol of pol λ; 0.21 ( $\pm$ 0.02) pmol of RP-A/0.5 pmol of pol λ and 0.73 ( $\pm$ 0.06) pmol RP-A/1.5 pmol of pol λ. In all cases 50% inhibition was reached at RP-A concentrations close to half of the pol λ input. This effect was specific for RP-A, since addition of PCNA, a protein also interacting with pol λ, did not affect dGTP misincorporation (Figure 4C, lanes 10–14), even in the presence of limiting amounts (0.2 pmol) of pol λ. BSA as a further control protein did not affect misincorporation by pol λ (Figure 4C, lanes 15–18). We have also shown earlier that substitution of RP-A with the prokaryotic ssDNA binding protein (*Escherichia coli* SSB) completely inhibited the activity of pol λ even in the presence of the correct nucleotide (18). In summary our results showed the critical role of a precise stoichiometry between pol λ and RP-A in order to allow inhibition of misincorporation, suggesting a

functional interaction between pol λ and RP-A in preventing mutagenesis.

#### RP-A specifically decreases the affinity of pol λ for mismatched nucleotides

Finally, the apparent binding constants of all four dNTPs to pol λ were determined with both a polypurinic and a polypyrimidinic primer/template [homopolymers (dT)<sub>16</sub>/(dA)<sub>200</sub> and (dA)<sub>16</sub>/(dT)<sub>200</sub>, respectively], in the presence of increasing amounts of RP-A and of 1 mM  $Mg^{++}$ . RP-A decreased the apparent affinities of pol λ for the incorrect nucleotides on both substrates, but without affecting the binding of the correct nucleotide (Table 1). Interestingly, no significant effects of RP-A were noted on the apparent rates of incorporation ( $k_{cat}$ ).

#### The intrinsic mutator phenotype of DNA polymerase λ is not affected by the combination of $Mn^{++}$ and $Mg^{++}$ over a wide range of molar ratios

In the cell, both  $Mg^{++}$  and  $Mn^{++}$  are present, and the intracellular concentration of  $Mg^{++}$  is generally assumed to be higher



than that of  $Mn^{++}$ . Since both these divalent cations can be used as cofactors for DNA synthesis by pol  $\lambda$ , but they differently affect its misincorporation ability, we investigated the effects of the combination of both  $Mg^{++}$  and  $Mn^{++}$  at various molar/molar (M/M) ratios. We have previously shown that the apparent binding affinity of pol  $\lambda$  for  $Mg^{++}$  and  $Mn^{++}$  is similar (in the range of 0.3–0.4 mM), but its catalytic activity is inhibited by  $Mg^{++}$  concentrations higher than 1–2 mM (11). We have determined the kinetic parameters for correct (dTTP) and incorrect (dATP or dGTP) incorporation on  $(dT)_{16}/(dA)_{200}$  as the template, in the presence of a fixed  $Mn^{++}$  concentration of 0.1 mM and increasing  $Mg^{++}$  concentrations in the reaction, resulting in  $Mn^{++}/Mg^{++}$  molar ratios of 1/1, 1/5 and 1/20, respectively. As shown in Figure 5A, up to a  $Mn^{++}/Mg^{++}$  molar ratio of 1:5, the incorp-

oration efficiencies ( $k_{cat}/K_m$  values) for both correct and incorrect nucleotides were comparable with the ones obtained in the presence of  $Mn^{++}$  alone. When the molar excess of  $Mg^{++}$  over  $Mn^{++}$  was increased up to a 1:20, the incorporation values decreased and approached those observed in the presence of  $Mg^{++}$  only. However, since the catalytic efficiency for both correct and incorrect incorporation were affected at the same level, no significant effects on the misincorporation ability of pol  $\lambda$  were observed over the range of different  $Mn^{++}/Mg^{++}$  molar ratios tested, as indicated by the small variations in the corresponding fidelity values for dATP and dGTP misincorporation shown in Figure 5B.

These results indicate that the intrinsic mutator phenotype of pol  $\lambda$  is maintained over a wide range of  $Mn^{++}/Mg^{++}$  molar ratios, a situation likely to occur also in the cellular environment.

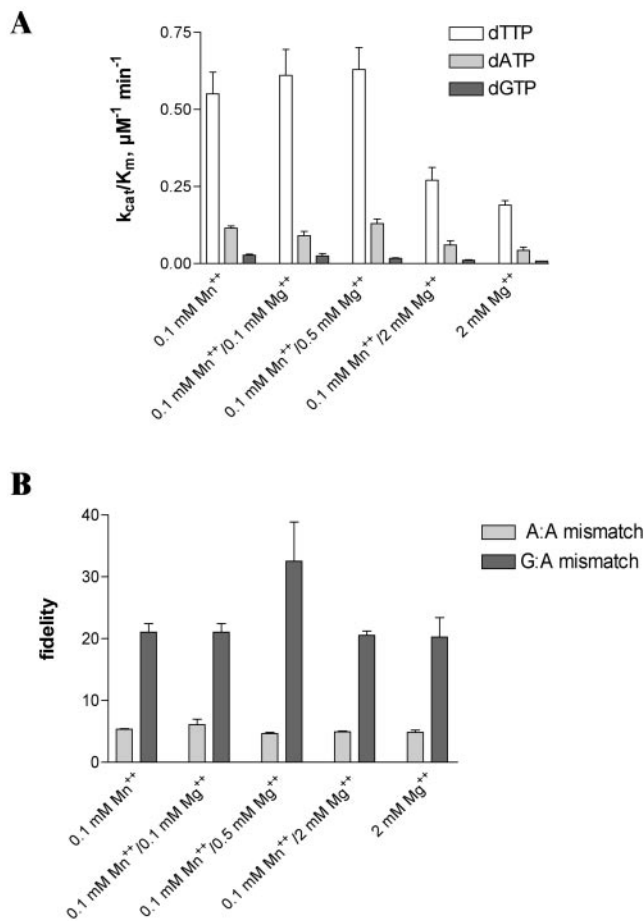


**Figure 5.** (A) The intrinsic mutator phenotype of pol  $\lambda$  is not affected by the combination of  $Mn^{++}$  and  $Mg^{++}$  over a wide range of molar ratios. Incorporation of dTTP, dATP or dGTP were monitored in the presence of 100 nM  $(dT)_{16}/(dA)_{200}$  and 50 nM pol  $\lambda$ , under the reactions conditions described in Materials and Methods. Kinetic parameters ( $k_{cat}$ ,  $K_m$ ,  $k_{cat}/K_m$  and  $1/f$ ) were determined as described in Materials and Methods. Nucleotide concentrations used were 0.5, 2.5, 10, 20 and 100  $\mu M$ , respectively. A. Incorporation efficiencies ( $k_{cat}/K_m$ ) values for dTTP (white bars), dATP (light grey bars) and dGTP (dark grey bars), were determined in the presence of 0.1 mM  $Mn^{++}$ , either alone or in combination with 0.1, 0.5 or 2 mM  $Mg^{++}$  respectively, or in the presence of 2 mM  $Mg^{++}$  alone. (B) Fidelity values for dATP (light grey bars) and dGTP (dark grey bars) misincorporation on  $(dT)_{16}/(dA)_{200}$ , expressed as the reciprocal of the misincorporation frequency ( $f$ ), calculated from the  $k_{cat}/K_m$  values shown in panel A, as described in Materials and Methods.

## DISCUSSION

In this study, the role of PCNA and RP-A on the *in vitro* fidelity of a family X pol in general and of pol  $\lambda$  in particular was for the first time analyzed and our results suggest a novel role for RP-A in suppressing the dangerous mutator phenotype of pol  $\lambda$ . First, we found that pol  $\lambda$  could incorporate rNTPs in the presence of nearly physiological concentrations of both  $Mn^{++}$  and  $Mg^{++}$ . Second, both the frequency and efficiency of mismatch generation by pol  $\lambda$  were influenced by the DNA sequence context, since on polypurine tracts the error rate of pol  $\lambda$  increased up to  $2.5 \times 10^{-1}$ . Third, PCNA had no influence on pol  $\lambda$  misincorporation. Fourth, the single stranded DNA binding protein RP-A selectively prevented mismatch generation by pol  $\lambda$ , without affecting correct base pair formation. This effect was not depending on the particular kind of mismatch, since we observed it for A:A, G:G and G:T mismatches. Fifth, a precise stoichiometry between the pol  $\lambda$  and RP-A was required. The observed effect was also specific for RP-A, since BSA or PCNA did not have any effect, whereas *E.coli* SSBs unspecifically inhibited correct nucleotide incorporation by pol  $\lambda$  (18 and data not shown).

Biochemical data suggested that  $Mn^{++}$  could play a role in DNA synthesis by pol  $\lambda$  *in vivo*.  $Mn^{++}$  favours misincorporation of deoxy- and ribonucleotides by pol  $\lambda$  compared with  $Mg^{++}$ . This is in agreement with the fact that  $Mn^{++}$  is known to relax base-pairing specificity and to increase tolerance for substrates more than  $Mg^{++}$  in the case of a number of pols (25). The steady-state kinetic analysis presented here allowed to calculate incorporation frequencies values for the most favoured misincorporation events in the range of  $10^{-2}$ – $10^{-3}$  and a strong preference of pol  $\lambda$  for the G:T and for the G:G mismatches. These results are consistent with pre-steady-state kinetic studies with a truncated form of pol  $\lambda$  (13).

Previous studies have shown that addition of PCNA increased the *in vitro* misincorporation rate of pol  $\delta$  (26,27), whereas combination of both RP-A and PCNA slightly increased the misincorporation rate of the family Y pols  $\eta$ ,  $\iota$  and  $\kappa$  (28–30). RP-A alone was shown to increase the fidelity of pol  $\alpha$ , an enzyme essential for DNA replication (31). We observed that PCNA alone had no effect on the fidelity of pol  $\lambda$ , even though these two proteins interact, whereas RP-A,

either alone or in combination with PCNA reduced its misincorporation, suggesting that PCNA and RP-A can differentially modulate the misincorporation abilities of different pols.

The increase in fidelity of pol  $\lambda$ , induced by RP-A was due to a decreased binding affinity of the mismatched nucleotides to the polymerase. In the steady-state approach used, this likely reflected a slower rate of formation of a ternary complex between pol  $\lambda$  bound to the primer and the incoming nucleotide. It is conceivable that the ternary complex of pol  $\lambda$  with the primer and a mismatched nucleotide is unstable and thus undergoes rapid dissociation. On the other hand, a ternary complex formed in the presence of a correct nucleotide is readily converted into its catalytically competent form, leading to incorporation. It is possible that RP-A could further destabilize pol  $\lambda$  from the primer/template junction when a mismatched nucleotide is bound, whereas the ternary complex formed in the presence of a correct nucleotide is stable enough to survive in the presence of RP-A. This mechanism could also explain the requirement of a precise stoichiometric ratio between pol  $\lambda$  and RP-A, since both proteins have to be present together at the same time in a complex with the primer/template and the nucleotide.

What could be the implications of these findings for the *in vivo* functions of pol  $\lambda$ ? Pol  $\lambda$ , together with pol  $\mu$ , is believed to synthesise short tracts of DNA during the NHEJ-mediated DSB repair (3). We show here that pol  $\lambda$ , similarly to pol  $\mu$ , can incorporate rNTPs in the presence of either  $Mn^{++}$  or  $Mg^{++}$ . Owing to the asymmetric nature of the NHEJ process, incorporation of rNTPs on one strand might mark it for further processing. In addition, since RNA:DNA base pairs are more stable than standard DNA:DNA base pairs, incorporation of rNTPs might help to stabilize the limited strand annealing required for the joining reaction of NHEJ (32).

In the presence of purine-rich regions (e.g. polyadenine tracts), the error rate of pol  $\lambda$  might be as high as one mistake every 5–12 incorporation events. This would result in pathologically high rates of transversions and transitions events during the resynthesis step of NHEJ. It has been shown that RP-A facilitated rejoining of non-homologous broken DNA ends and that depletion of RP-A from cell extracts reduced the efficiency of the *in vitro* NHEJ reaction (33). Since RP-A can specifically reduce the misincorporation rate of pol  $\lambda$ , we propose that RP-A has a novel role in keeping the undesired mutator phenotype of pol  $\lambda$  under control during NHEJ.

It has been proposed that a replication fork stalled at an abasic site might be rescued by pol  $\lambda$ , which synthesises a short DNA tract encompassing the lesion, thus creating a new 3'-OH end available for elongation by the replicative pols (4,5). RP-A is normally accumulated at single strand DNA regions and could, therefore, limit the possibility of introducing mistakes by pol  $\lambda$ .

Finally, a recent result showed that pol  $\lambda$  physically interacts with the oxidative DNA damage-specific glycosylase SMUG-1 and is recruited to repair sites *in vivo* (34). Oxidative DNA damage is normally repaired through base excision repair (BER). Short-patch BER requires incorporation of 1–2 nt and is mainly dependent on pol  $\beta$ , whereas long patch BER requires synthesis of longer tracts of DNA (7–10 nt). RP-A, along with PCNA, pol  $\delta$ , pol  $\epsilon$  or pol  $\beta$ , has been implicated in the long BER pathway. Since there is

evidence that pol  $\lambda$  is involved in back-up function in BER (35) it is tempting to note that during long patch BER pol  $\lambda$  has the probability to generate at least one misincorporation event, especially when a polypurine tract has to be copied. Purine nucleotides are very sensitive to base damaging agents. The resulting modified bases, e.g. 8<sup>oxo</sup>dG or 3<sup>met</sup>dA, can be repaired by BER. Therefore it is conceivable to hypothesize that polypurine tracts might be subjected to frequent DNA repair by BER. Thus, in this context the presence of RP-A might be essential in order to avoid unwarranted errors by pol  $\lambda$ .

## ACKNOWLEDGEMENTS

This work was supported by the Swiss National Science Foundation to G.M. (for a short term visit to the Institute of Veterinary Biochemistry and Molecular Biology) and to U.H. and by the Kanton of Zürich to U.H. and I.S.; by the EU project QLK3-CT-2002-02071 (G.M., U.H.); by the CARIPLO Foundation project 'Oncogenetica e Proteomica della Replicazione' (2003.1663/10.8441) to G.M.; by Grant 3477 from ARC to G.V. Funding to pay the Open Access publication charges for this article was provided by the EU project QLK3-CT-2002-02071 REPBIOTECH.

*Conflict of interest statement.* None declared.

## REFERENCES

- Hubscher,U., Maga,G. and Spadari,S. (2002) Eukaryotic DNA polymerases. *Annu Rev. Biochem.*, **71**, 133–163.
- Garcia-Diaz,M., Dominguez,O., Lopez-Fernandez,L.A., de Lera,L.T., Saniger,M.L., Ruiz,J.F., Parraga,M., Garcia-Ortiz,M.J., Kirchhoff,T., del Mazo,J. *et al.* (2000) DNA polymerase lambda (Pol lambda), a novel eukaryotic DNA polymerase with a potential role in meiosis. *J. Mol. Biol.*, **301**, 851–867.
- Ramadan,K., Shevelev,I. and Hubscher,U. (2004) The DNA-polymerase-X family: controllers of DNA quality? *Nat. Rev. Mol. Cell Biol.*, **5**, 1038–1043.
- Maga,G., Villani,G., Ramadan,K., Shevelev,I., Le Gac,N.T., Blanco,L., Blanca,G., Spadari,S. and Hubscher,U. (2002) Human DNA polymerase lambda functionally and physically interacts with proliferating cell nuclear antigen in normal and translesion DNA synthesis. *J. Biol. Chem.*, **277**, 48434–48440.
- Maga,G., Blanca,G., Shevelev,I., Frouin,I., Ramadan,K., Spadari,S., Villani,G. and Hubscher,U. (2004) The human DNA polymerase lambda interacts with PCNA through a domain important for DNA primer binding and the interaction is inhibited by p21/WAF1/CIP1. *Faseb J.*, **18**, 1743–1745.
- Lee,J.W., Blanco,L., Zhou,T., Garcia-Diaz,M., Bebenek,K., Kunkel,T.A., Wang,Z. and Povirk,L.F. (2004) Implication of DNA polymerase lambda in alignment-based gap filling for nonhomologous DNA end joining in human nuclear extracts. *J. Biol. Chem.*, **279**, 805–811.
- Ma,Y., Lu,H., Tippin,B., Goodman,M.F., Shimazaki,N., Koivai,O., Hsieh,C.L., Schwarz,K. and Lieber,M.R. (2004) A biochemically defined system for mammalian nonhomologous DNA end joining. *Mol. Cell*, **16**, 701–713.
- McElhinny,S.A., Havener,J.M., Garcia-Diaz,M., Juarez,R., Bebenek,K., Kee,B.L., Blanco,L., Kunkel,T.A. and Ramsden,D.A. (2005) A gradient of template dependence defines distinct biological roles for family X polymerases in nonhomologous end joining. *Mol. Cell*, **19**, 357–366.
- DeRose,E.F., Kirby,T.W., Mueller,G.A., Bebenek,K., Garcia-Diaz,M., Blanco,L., Kunkel,T.A. and London,R.E. (2003) Solution structure of the lyase domain of human DNA polymerase lambda. *Biochemistry*, **42**, 9564–9574.

10. Garcia-Diaz,M., Bebenek,K., Krahn,J.M., Blanco,L., Kunkel,T.A. and Pedersen,L.C. (2004) A structural solution for the DNA polymerase lambda-dependent repair of DNA gaps with minimal homology. *Mol. Cell*, **13**, 561–572.
11. Blanca,G., Shevelev,I., Ramadan,K., Villani,G., Spadari,S., Hubscher,U. and Maga,G. (2003) Human DNA polymerase lambda diverged in evolution from DNA polymerase beta toward specific Mn(++) dependence: a kinetic and thermodynamic study. *Biochemistry*, **42**, 7467–7476.
12. Ramadan,K., Shevelev,I.V., Maga,G. and Hubscher,U. (2002) DNA polymerase lambda from calf thymus preferentially replicates damaged DNA. *J. Biol. Chem.*, **277**, 18454–18458.
13. Fiala,K.A., Abdel-Gawad,W. and Suo,Z. (2004) Pre-steady-state kinetic studies of the fidelity and mechanism of polymerization catalyzed by truncated human DNA polymerase lambda. *Biochemistry*, **43**, 6751–6762.
14. Werneburg,B.G., Ahn,J., Zhong,X., Hondal,R.J., Kraynov,V.S. and Tsai,M.D. (1996) DNA polymerase beta: pre-steady-state kinetic analysis and roles of arginine-283 in catalysis and fidelity. *Biochemistry*, **35**, 7041–7050.
15. Roettger,M.P., Fiala,K.A., Sompalli,S., Dong,Y. and Suo,Z. (2004) Pre-steady-state kinetic studies of the fidelity of human DNA polymerase mu. *Biochemistry*, **43**, 13827–13838.
16. Bebenek,K., Garcia-Diaz,M., Blanco,L. and Kunkel,T.A. (2003) The frameshift infidelity of human DNA polymerase lambda. Implications for function. *J. Biol. Chem.*, **278**, 34685–34690.
17. Blanca,G., Villani,G., Shevelev,I., Ramadan,K., Spadari,S., Hubscher,U. and Maga,G. (2004) Human DNA polymerases lambda and beta show different efficiencies of translesion DNA synthesis past abasic sites and alternative mechanisms for frameshift generation. *Biochemistry*, **43**, 11605–11615.
18. Maga,G., Ramadan,K., Locatelli,G.A., Shevelev,I., Spadari,S. and Hubscher,U. (2005) DNA elongation by the human DNA polymerase lambda polymerase and terminal transferase activities are differentially coordinated by proliferating cell nuclear antigen and replication protein A. *J. Biol. Chem.*, **280**, 1971–1981.
19. Shevelev,I., Blanca,G., Villani,G., Ramadan,K., Spadari,S., Hubscher,U. and Maga,G. (2003) Mutagenesis of human DNA polymerase lambda: essential roles of Tyr505 and Phe506 for both DNA polymerase and terminal transferase activities. *Nucleic Acids Res.*, **31**, 6916–6925.
20. Jonsson,Z.O., Hindges,R. and Hübscher,U. (1998) Regulation of DNA replication and repair proteins through interaction with the front side of proliferating cell nuclear antigen. *EMBO J.*, **17**, 2412–2425.
21. Henricksen,L.A., Umbricht,C.B. and Wold,M.S. (1994) Recombinant replication protein A: expression, complex formation, and functional characterization. *J. Biol. Chem.*, **269**, 11121–11132.
22. Malecki,E.A., Devenyi,A.G., Beard,J.L. and Connor,J.R. (1999) Existing and emerging mechanisms for transport of iron and manganese to the brain. *J. Neurosci. Res.*, **56**, 113–122.
23. Bergoglio,V., Ferrari,E., Hubscher,U., Cazaux,C. and Hoffmann,J.S. (2003) DNA polymerase beta can incorporate ribonucleotides during DNA synthesis of undamaged and CPD-damaged DNA. *J. Mol. Biol.*, **331**, 1017–10123.
24. Ruiz,J.F., Juarez,R., Garcia-Diaz,M., Terrados,G., Picher,A.J., Gonzalez-Barrera,S., Fernandez de Henestrosa,A.R. and Blanco,L. (2003) Lack of sugar discrimination by human Pol mu requires a single glycine residue. *Nucleic Acids Res.*, **31**, 4441–4449.
25. Vaisman,A., Ling,H., Woodgate,R. and Yang,W. (2005) Fidelity of Dpo4: effect of metal ions, nucleotide selection and pyrophosphorolysis. *EMBO J.*, **24**, 2957–2967.
26. Mozzherin,D.J., McConnell,M., Jasko,M.V., Krayevsky,A.A., Tan,C.K., Downey,K.M. and Fisher,P.A. (1996) Proliferating cell nuclear antigen promotes misincorporation catalyzed by calf thymus DNA polymerase delta. *J. Biol. Chem.*, **271**, 31711–31717.
27. Mozzherin,D.J., Shibutani,S., Tan,C.K., Downey,K.M. and Fisher,P.A. (1997) Proliferating cell nuclear antigen promotes DNA synthesis past template lesions by mammalian DNA polymerase delta. *Proc. Natl Acad. Sci. USA*, **94**, 6126–6131.
28. Haracska,L., Johnson,R.E., Unk,I., Phillips,B., Hurwitz,J., Prakash,L. and Prakash,S. (2001) Physical and functional interactions of human DNA polymerase eta with PCNA. *Mol. Cell Biol.*, **21**, 7199–7206.
29. Haracska,L., Johnson,R.E., Unk,I., Phillips,B.B., Hurwitz,J., Prakash,L. and Prakash,S. (2001) Targeting of human DNA polymerase iota to the replication machinery via interaction with PCNA. *Proc. Natl Acad. Sci. USA*, **98**, 14256–14261.
30. Haracska,L., Unk,I., Johnson,R.E., Phillips,B.B., Hurwitz,J., Prakash,L. and Prakash,S. (2002) Stimulation of DNA synthesis activity of human DNA polymerase kappa by PCNA. *Mol. Cell Biol.*, **22**, 784–791.
31. Maga,G., Frouin,I., Spadari,S. and Hübscher,U. (2001) RP-A as a fidelity clamp for DNA polymerase alpha. *J. Biol. Chem.*, **276**, 18235–18242.
32. Ma,Y., Lu,H., Schwarz,K. and Lieber,M.R. (2005) Repair of double-strand DNA breaks by the human nonhomologous DNA end joining pathway: the iterative processing model. *Cell Cycle*, **4**, 1193–1200.
33. Perrault,R., Cheong,N., Wang,H. and Iliakis,G. (2001) RPA facilitates rejoining of DNA double-strand breaks in an in vitro assay utilizing genomic DNA as substrate. *Int. J. Radiat. Biol.*, **77**, 593–607.
34. Braithwaite,E.K., Kedar,P.S., Lan,L., Polosina,Y.Y., Asagoshi,K., Poltoratsky,V.P., Horton,J.K., Miller,H., Teebor,G.W. et al. (2005) DNA polymerase lambda protects mouse fibroblasts against oxidative DNA damage and is recruited to sites of DNA damage/repair. *J. Biol. Chem.*, **280**, 31641–31647.
35. Braithwaite,E.K., Prasad,R., Shock,D.D., Hou,E.W., Beard,W.A. and Wilson,S.H. (2005) DNA polymerase lambda mediates a back-up base excision repair activity in extracts of mouse embryonic fibroblasts. *J. Biol. Chem.*, **280**, 18469–18475.